Measurements of the Higgs boson inclusive and differential fiducial cross sections in the four-lepton decay channel with the ATLAS detector using partial Run 3 data

Elena Cuppini

Higgs Hunting 2026, 16th of September

ATLAS EXPERIMENT

MAX-PLANCK-INSTITUT FÜR PHYSIK

The $H \rightarrow ZZ^{*} \rightarrow 4\ell$ Channel

- The Higgs boson couples to all known fundamental particles with mass, including itself
- $H \rightarrow ZZ^{*} \rightarrow 4\ell$ channel characterised by a final state containing two pairs of oppositely charged leptons from the same primary vertex
  - Four possible final states: **4μ, $4e$, $2e2\mu$, $2\mu2e$**
  - Excellent mass resolution and high signal-to-background ratio (~2)
  - From discovery to precision measurements!

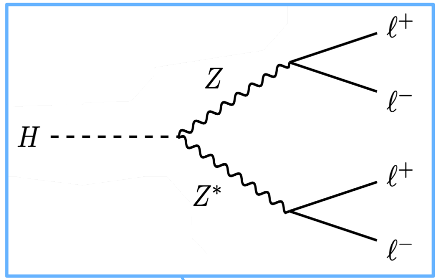

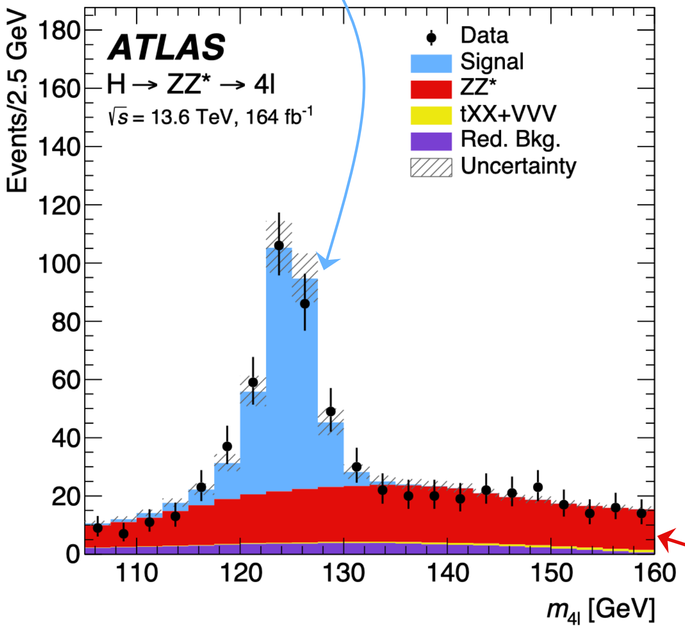

Background Estimation

Irreducible Background: qq- and ggZZ^{*}

- Semi-data driven estimate: floating ZZ^{*} normalisation factor extracted from $m_{4\ell}$ sidebands [105-115], [130-160] GeV

Reducible Background: Z+jets, $t\bar{t}$, and WZ

- At least 1 non-prompt lepton: contribution estimated through data-driven **fake factor method**

Minor Backgrounds: $t\bar{t}+X$, VVV, estimated from simulation

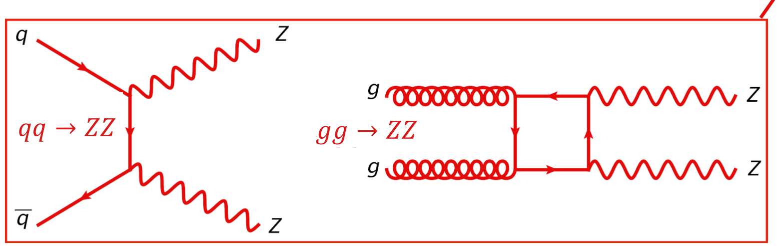

Cross-section measurements with partial Run 3 data

ATLAS dataset for partial Run 3 (2022-2024) corresponds to an integrated luminosity of **164 fb^{-1}** of $\sqrt{s}$ = **13.6** TeV

- Great chance to perform cross-section measurements in $\mathbf{H \rightarrow ZZ^* \rightarrow 4\ell}$ with a dataset of a similar size to full Run 2!

Inclusive and **differential fiducial**, as well as **total** cross-section measurements in $\mathbf{H \rightarrow ZZ^* \rightarrow 4\ell}$, using the partial Run 3 ATLAS dataset (JHEP 08 (2026) 052)

- Analysis strategy largely follows the one implemented for the Run 2 measurements
  - **Differential fiducial cross-section** for:
    - Higgs kinematics ($p_T^{4\ell}$, $y_{4\ell}$)
    - Jet variables (N_{jets}, $\Delta\phi_{jj}$)
    - Decay-side observables
      - m_{12}, m_{34}, the invariant masses of the on- and off-shell Z bosons
      - ϕ, angle between the decay planes of the two Z bosons
    - **New** 2D variable $p_T^{4\ell}$ **vs** m_{34}
  - **And their interpretation!**
    - Standard Model Effective Field Theory (SMEFT) interpretation of differential cross section distributions sensitive to CP-even/odd HVV couplings

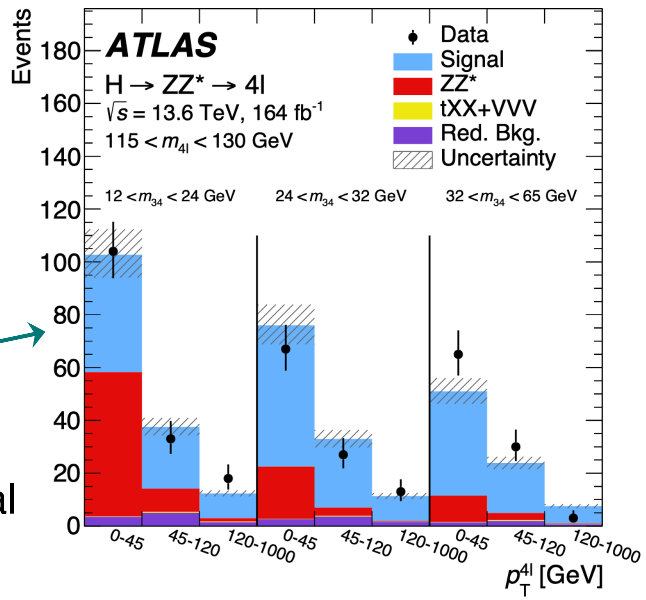

Analysis Strategy

- **Fiducial cross-section $\boldsymbol{\sigma_j^{fid}}$** per differential **bin $\boldsymbol{j}$** is extracted using a binned maximum-likelihood fit of the signal and background templates to the observed $\boldsymbol{m_{4\ell}}$ spectrum
- Fit performed separately in each reconstruction bin i of the corresponding differential observable

$$N_i\,(m_{4\ell}) = \sum_j \sigma_j^{\mathrm{fid}} \cdot \mathscr{P}_i\,(m_{4\ell}) \cdot r_{ij} \cdot (1 + f_i^{\mathrm{nonfid}}) \cdot \mathscr{L} + N_i^{\mathrm{bkg}}\,(m_{4\ell})$$

$\sigma_j^{\mathrm{fid}} = \sigma_j \cdot A_j \cdot \mathscr{B}$ = parameter of interest

$\mathscr{P}_i(m_{4\ell})$ = $m_{4\ell}$ signal shape

$N_i^{\mathrm{bkg}}(m_{4\ell})$ = background contribution

r_{ij} = detector response matrix (or fiducial efficiency ϵ_i in the inclusive measurement)

f_i^{nonfid} = fiducial leakage (Fraction of events outside the fiducial region which are reconstructed in the signal region)

- Detector response matrices determined from simulation for each differential variable used to unfold to the fiducial phase-space

- ZZ^* yields are constrained directly from data by including $m_{4\ell}$ sideband regions [105, 115] ∪ [130, 160] GeV in the likelihood fit

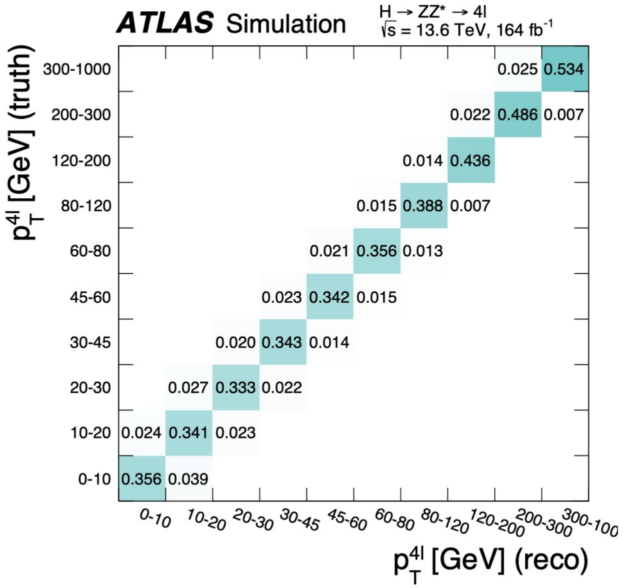

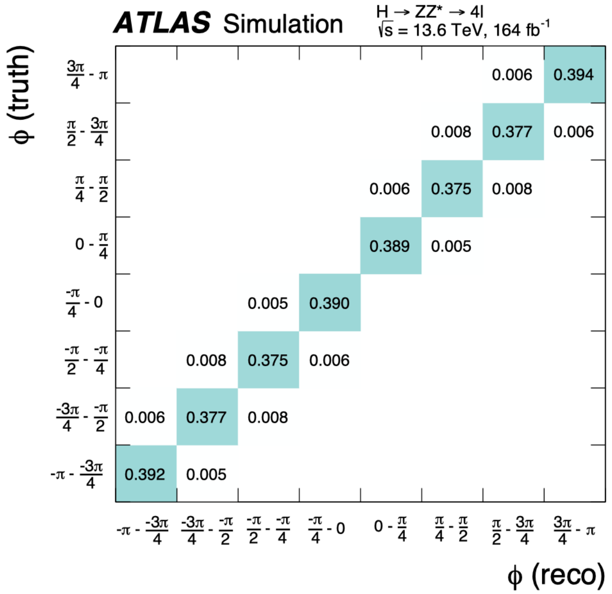

Inclusive Fiducial Cross-Section Measurements

- Observed number of events is comparable to the expected signal and background yields for each of the four-lepton final states (4μ, $4e$, $2e2\mu$, $2\mu2e$):

Final state	Signal	ZZ^*	Other Backgrounds	Total SM	Observed
4μ	90.5 ± 5.3	41.2 ± 1.6	4.5 ± 0.3	136 ± 6	136
$2e2\mu$	63.4 ± 4.0	30.0 ± 1.3	4.7 ± 0.5	98 ± 5	98
$2\mu2e$	40.7 ± 9.1	15.6 ± 4.4	5.6 ± 0.2	62 ± 13	67
$4e$	36.5 ± 9.2	14.1 ± 4.3	5.3 ± 0.3	56 ± 13	59
Total	231 ± 23	101 ± 10	20.1 ± 1.3	352 ± 32	360

- **Observed (expected) inclusive fiducial cross-section** extracted from the $m_{4\ell}$ fit:

$$\sigma_{\mathrm{comb}} = 3.65 \pm 0.30\ (\mathrm{stat.})\ ^{+0.18}_{-0.16}\ (\mathrm{sys.})\ \mathrm{fb} = 3.65\ ^{+0.35}_{-0.33}\ \mathrm{fb}$$

$$\sigma^{\mathrm{SM}}_{\mathrm{comb}} = 3.68 \pm 0.17\ \mathrm{fb}$$

- Total cross-section extrapolated from the inclusive XS

$$\sigma_{\mathrm{total}} = 59.3 \pm 4.8\ (\mathrm{stat.}) \pm 3.1\ (\mathrm{sys.})\ \mathrm{pb} = 59.3 \pm 5.7\ \mathrm{pb}$$

$$\sigma^{\mathrm{SM}}_{\mathrm{total}} = 59.9 \pm 3.0\ \mathrm{pb}$$

Same precision as the full Run 2 measurement!

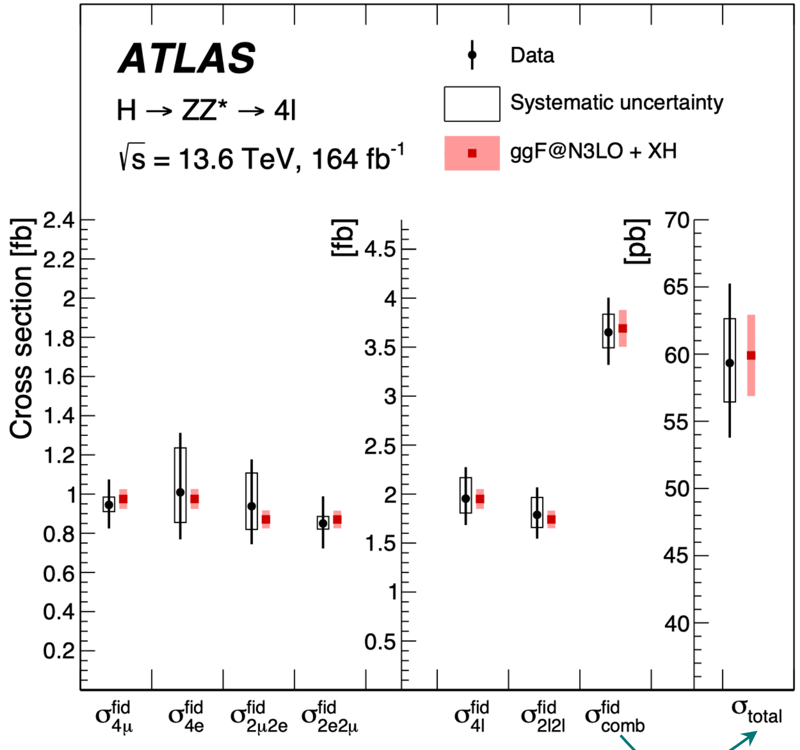

$$\sigma^{\mathrm{fid}}_{\mathrm{comb}} = \sigma_{\mathrm{total}} \cdot A \cdot \mathscr{B}$$

- Systematic uncertainty dominated by lepton reconstruction and isolation efficiencies

Differential Cross-Section Results

- Pre fit yields and differential fiducial cross-section measurements for $p_T^{4\ell}$ and ϕ
- **Good agreement with predicted XS observed across all bins**
  - MG5 and NNLO predictions normalised to the YR4 N3LO cross-section for ggF

$p_T^{4\ell}$

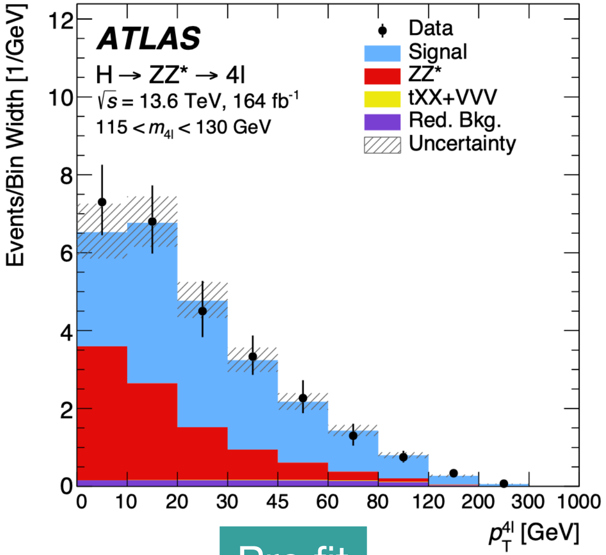

Pre fit

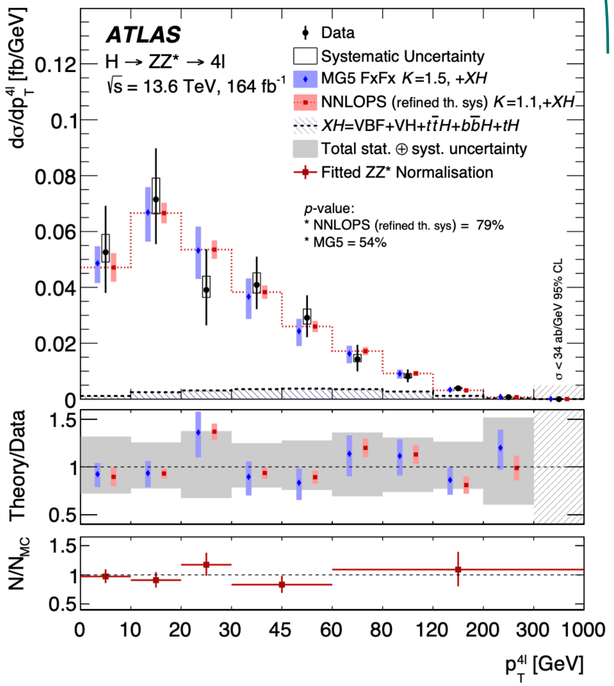

ϕ

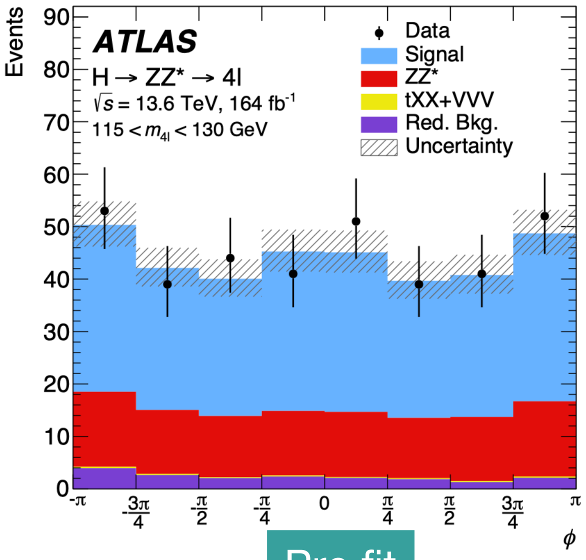

Pre fit

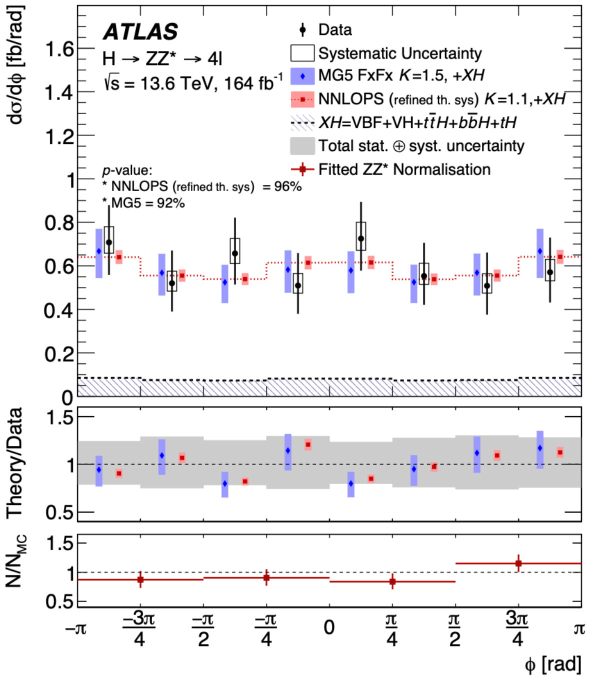

- Measurements are generally still statistical dominated. Dominant systematics are primarily from lepton efficiency and (for jet-related variables) jet energy calibration uncertainties

SMEFT Interpretation - Introduction

- H $\rightarrow ZZ^* \rightarrow 4\ell$ is sensitive to Standard Model Effective Field Theory (SMEFT) **SMEFT** operators impacting **Higgs couplings to EW bosons** ($c_{\rm HW}$, $c_{\rm HWB}$, $c_{\rm HB}$, and their CP-odd counterparts)

$$\mathcal{L}_{\rm EFT} = \mathcal{L}_{\rm SM} + \sum_i \frac{C_i^{(d)}}{\Lambda^{(d-4)}} O_i^{(d)} \quad \text{for } d > 4$$

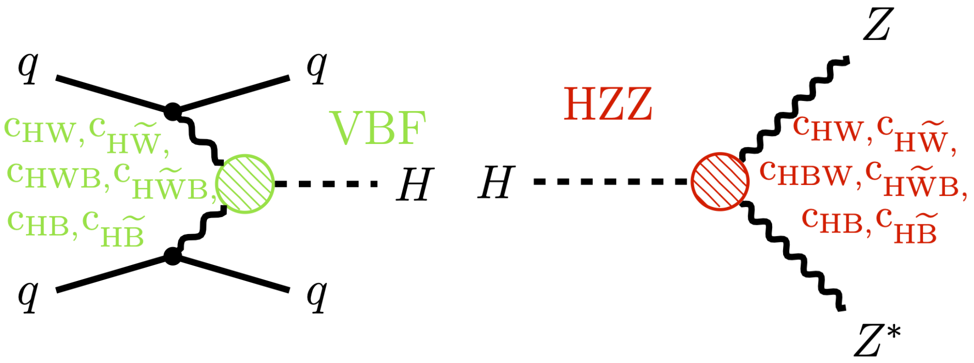

- Effective couplings **modify event kinematics** → probed using differential cross-section measurements
  - $\boldsymbol{\phi}$ and $\boldsymbol{p_T^{4\ell}}$ **vs** $\boldsymbol{m_{34}}$ shown to be the **most sensitive** to the probed EFT effects:
    - $\boldsymbol{\phi}$: significantly improves sensitivity to **linear EFT** terms (changes sign across ϕ → periodic modulation cancels in ϕ-inclusive distributions)
    - $\boldsymbol{p_T^{4\ell}}$ **vs** $\boldsymbol{m_{34}}$: captures EFT effects in both Higgs **production** ($p_T^{4\ell}$) and **decay** (m_{34}) vertices

- SMEFT Wilson coefficients (Warsaw basis) constrained by comparing the unfolded signal cross-section in each bin of the chosen distribution to the SMEFT expectation → Expected cross-section and acceptance parametrised in terms of WCs

SMEFT Interpretation - Results

Wilson coefficients are fitted one at a time (all others are set to zero) or two at a time:

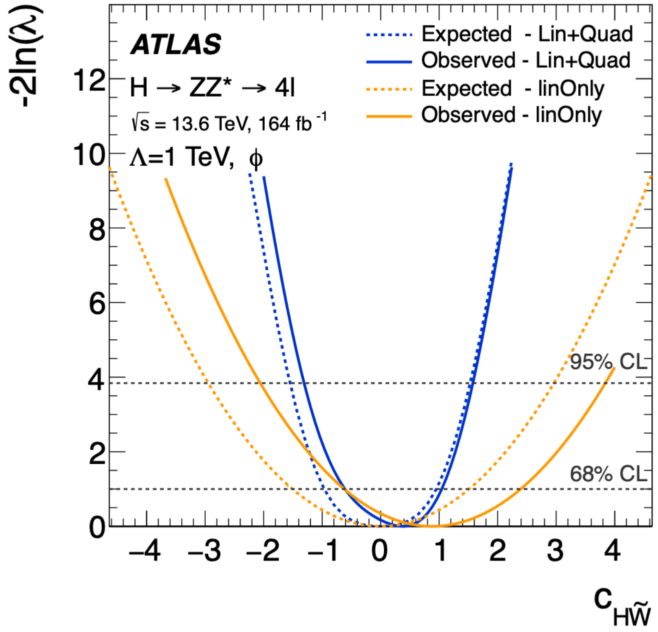

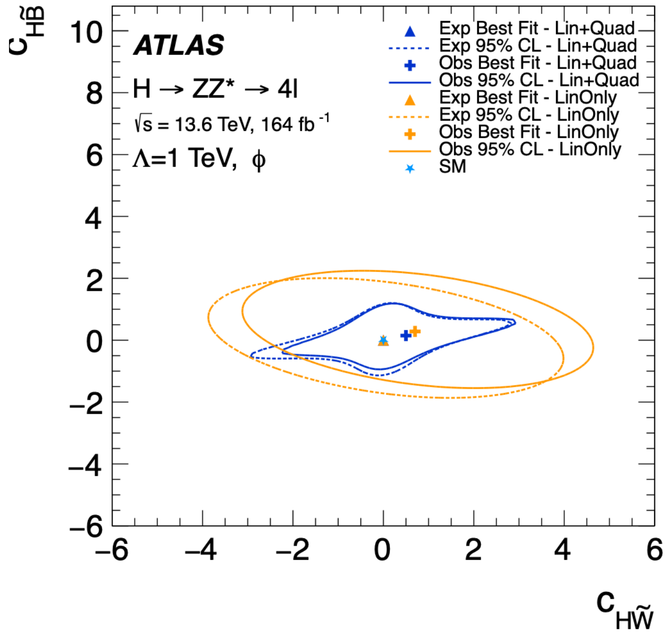

- Linear terms contribute substantially to the constraints → improvement in the robustness of the interpretation
- Inclusion of quadratic EFT terms tightens these constraints
- Possible improvements from more data + probing smaller values of Wilson coefficients

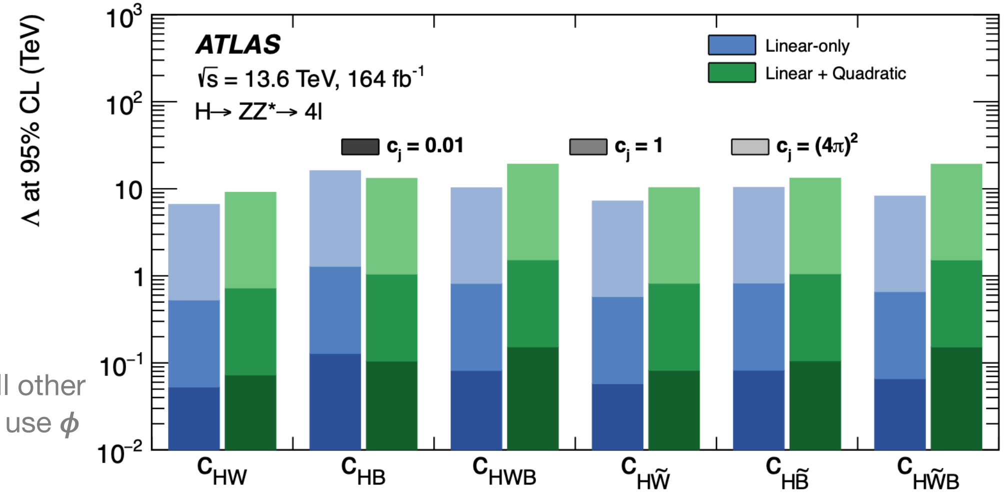

- All measured Wilson coefficients consistent with the SM expectation of 0
- Corresponding limits on the new physics scale Λ for benchmark coefficient values

Note: c_{HW} uses $p_T^{4\ell}$ vs. m_{34}, all other 1D limits (including CP-odd) use ϕ

Conclusions

- Higgs production cross-section measured at 13.6 TeV in the $H \rightarrow ZZ^* \rightarrow 4\ell$ channel at ATLAS using 164 fb^{-1} of data, both **inclusively** and for **eight differential variables** and their interpretation in terms of SMEFT
  - Results comparable with Run 2, with similar precision too
  - To summarise the novelties:
    - New **fake factor method** used for the reducible background estimation
    - New doubly differential one never measured before $p_T^{4\ell}$ **vs** m_{34}
    - Improved sensitivity to **linear EFT terms** from the interpretation of ϕ

➠All of this and more in JHEP 08 (2026) 052

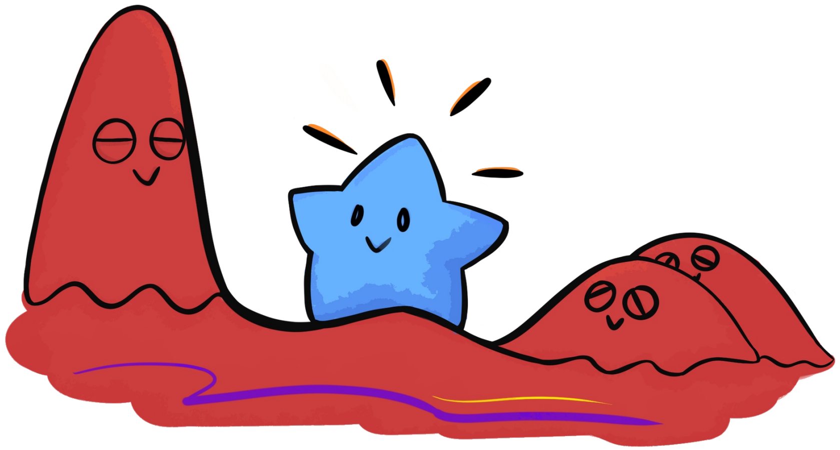

Thanks to Siyuan Yan (Glasgow) for the illustration!

Stay tuned for coming full Run3 results!

Backup

Fake Factor Method

Illustrations from Maximilian Goblirsch-Kolb and Jiawei Wang

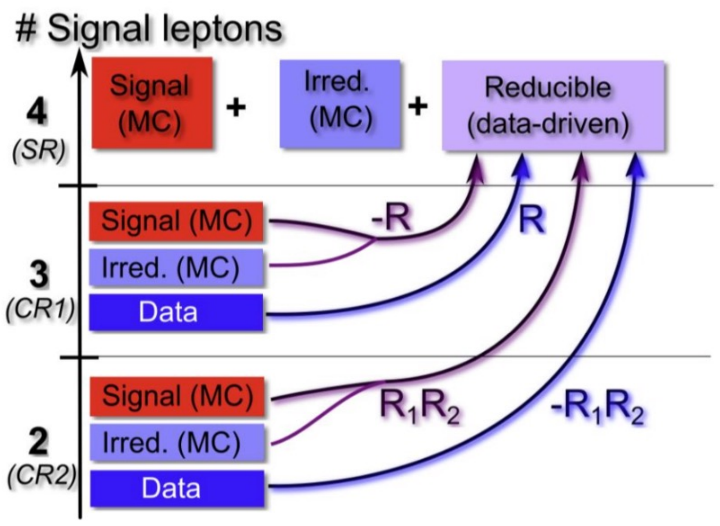

- **NEW** for this paper, the **fake factor method** is used for estimating the **reducible background**:
  - *Fakes* defined as leptons which pass the selection cuts, even though they should not
  - *Fake efficiency* eff_{fake} = fraction of non-prompt leptons passing isolation and impact parameter requirements

- Each event in the signal region weighted by a ***fake factor***(FF):

$$FF = eff_{fake}/(1-eff_{fake})$$

- FF evaluated from eff_{fake} in a 3D map of $p_T^{4\ell}$, $Njets$ and η in 2 control regions:
  - **CR Z:** **Z+jets** enriched
  - **CR top:** $t\bar{t}$ enriched

  → Final result uses a **combination** of CR Z and CR top
    - Systematic uncertainty added to covers this choice

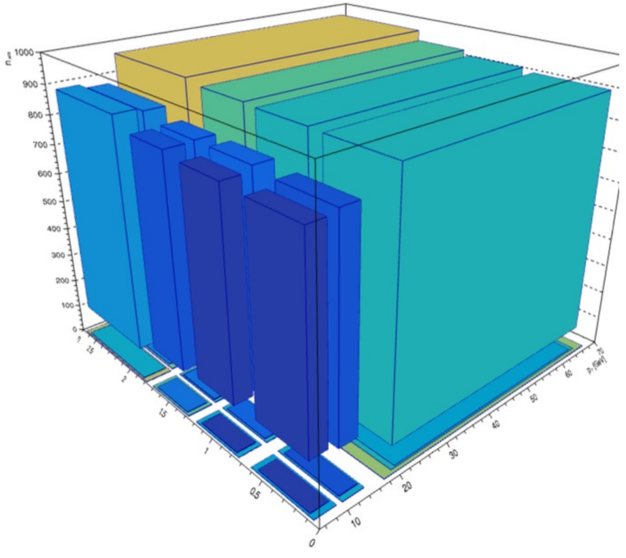

3D visualization of Fake Factors

arXiv:2211.16178
arXiv:2310.04350
arXiv:2308.12324

Fiducial Phase Space

- **Fiducial phase space** defined to closely match reco-level phase space
- Definition follows Run 2 and early Run 3 measurements

Leptons and jets	
Leptons	$p_T > 5$ GeV, $\|\eta\| < 2.7$
Jets	$p_T > 30$ GeV, $\|y\| < 4.4$
Lepton selection and pairing	
Lepton kinematics	$p_T > 20, 15, 10$ GeV
Leading pair (m_{12})	SFOC lepton pair with smallest $\|m_Z - m_{\ell\ell}\|$
Subleading pair (m_{34})	remaining SFOC lepton pair with smallest $\|m_Z - m_{\ell\ell}\|$
Event selection (at most one quadruplet per event)	
Mass requirements	50 GeV$< m_{12} <$ 106 GeV and 12 GeV$< m_{34} <$ 115 GeV
Lepton separation	$\Delta R(\ell_i, \ell_j) > 0.1$
Lepton/Jet separation	$\Delta R(\ell_i, \text{jet}) > 0.1$
J/ψ veto	$m(\ell_i, \ell_j) > 5$ GeV for all SFOC lepton pairs
If extra lepton with $p_T > 12$ GeV	Quadruplet with largest matrix element value
Mass window	105 GeV$< m_{4\ell} <$ 160 GeV

Reconstructed even-level yields

- Differential cross-sections are measured for variables which are **sensitive to both the production and decay** of the Higgs Boson: here, results for $p_T^{4\ell}$,N_{jets}, m_{34} and $y_{4\ell}$

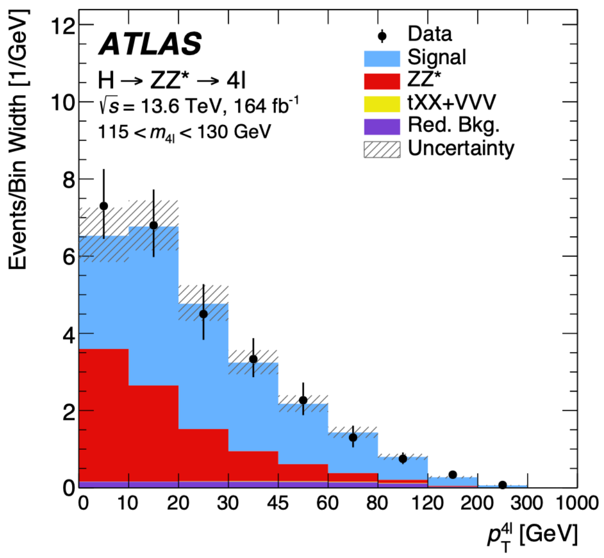

Information on Higgs production

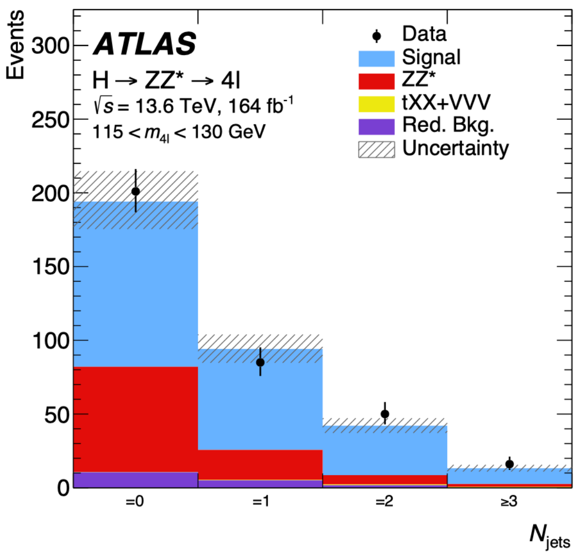

Information on Higgs production

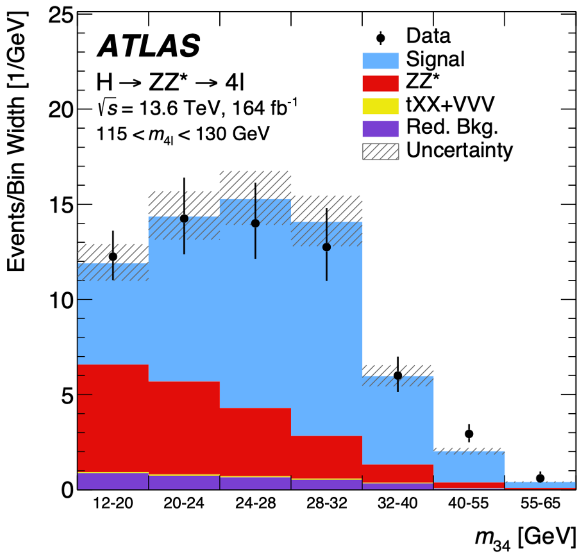

Information on Higgs decay + parity and spin of the Higgs, good for BSM interpretations

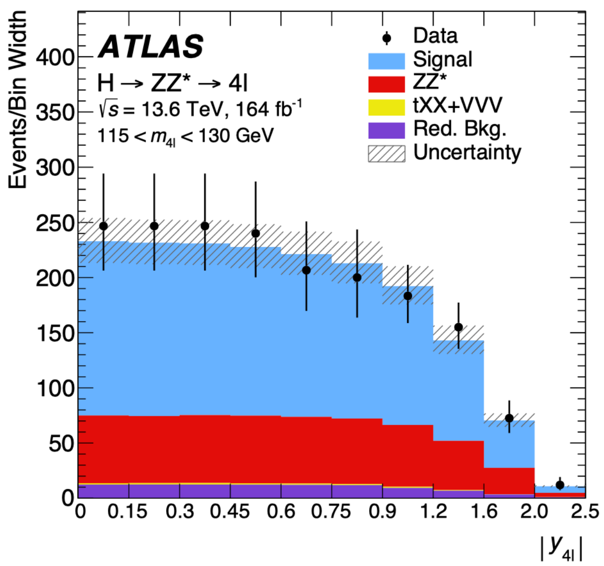

Constraint of the gluon Parton Distribution Function

Reconstructed even-level yields

- Differential cross-sections are measured for variables which are **sensitive to both the production and decay** of the Higgs Boson: here, results for m_{12}, $\Delta\phi_{jj}$, ϕ, and $p_T^{4\ell} m_{34}$

NEW!

Binning harmonised with interpretation team

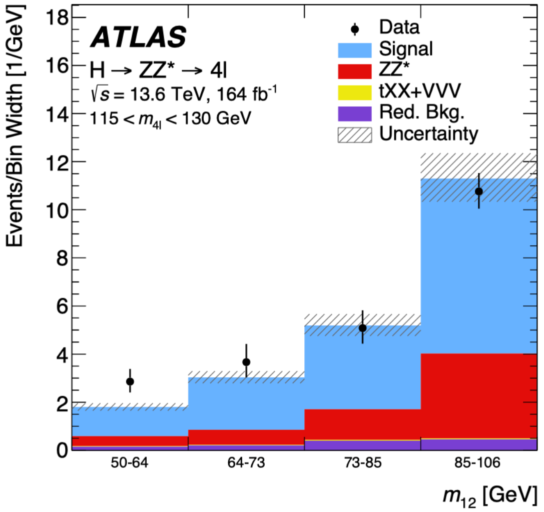

Information on Higgs decay + parity and spin of the Higgs

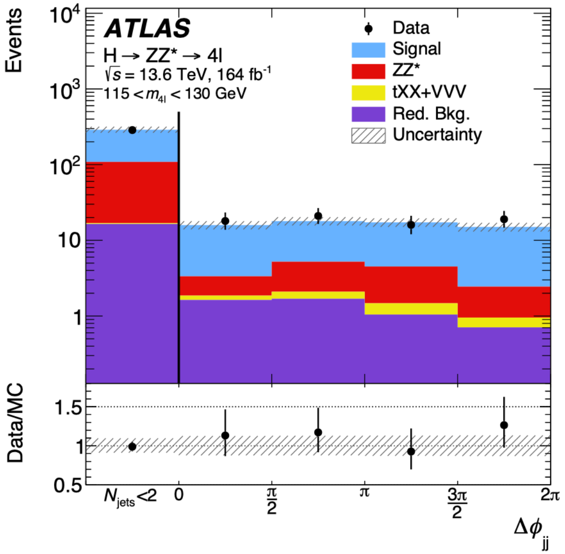

Sensitive to spin-CP effects

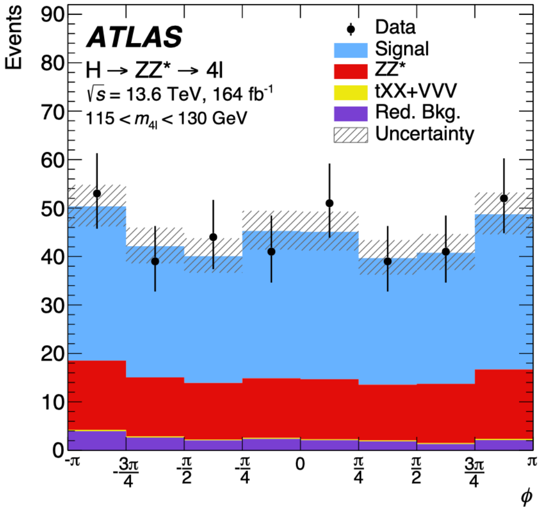

Sensitivity to the spin and parity of the Higgs

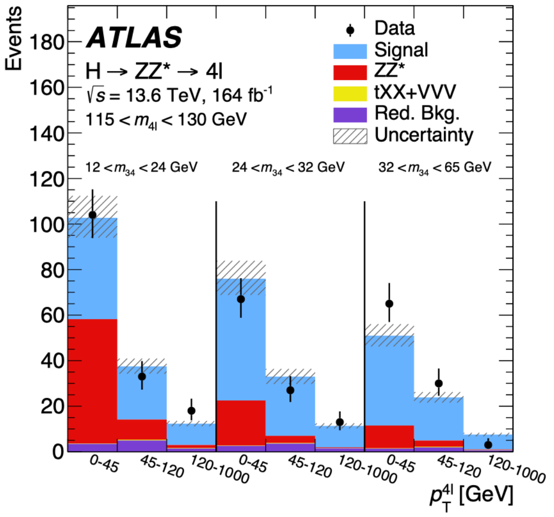

Information on Higgs production

From $p_T^{4\ell}$

+

Information on Higgs decay + parity and spin of the Higgs, good for BSM interpretations

From m_{34}

Response Matrices

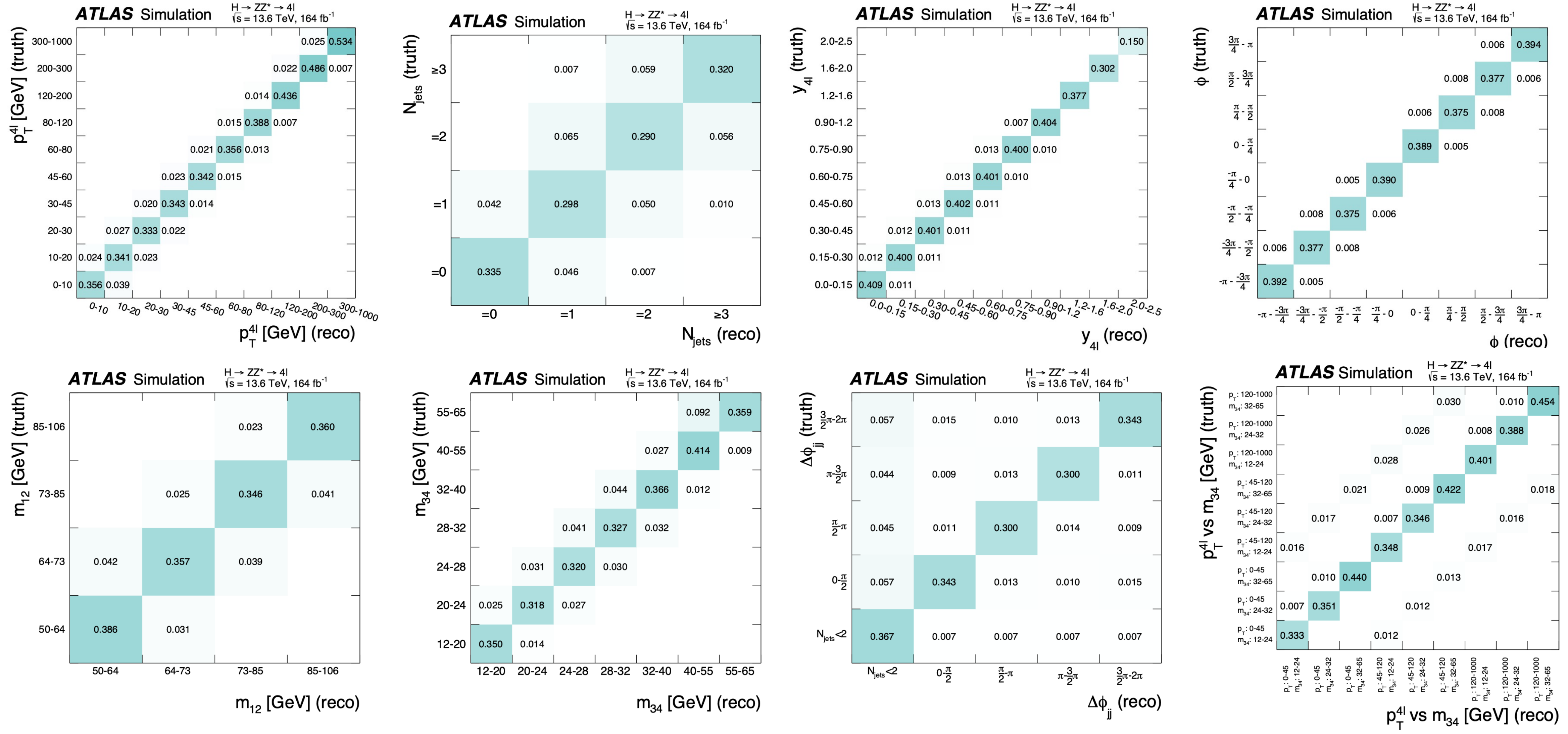

Differential Cross-Section Results

- Differential fiducial cross-section measurements for $p_T^{4\ell}$, N_{jets}, m_{12}, m_{34}, $y_{4\ell}$, $\Delta\phi_{\text{jj}}$, ϕ, and 2D $p_T^{4\ell}$ vs m_{34}
- **Good agreement with predicted XS observed across all bins**
  - MG5 and NNLO predictions normalised to the YR4 N3LO cross-section for ggF

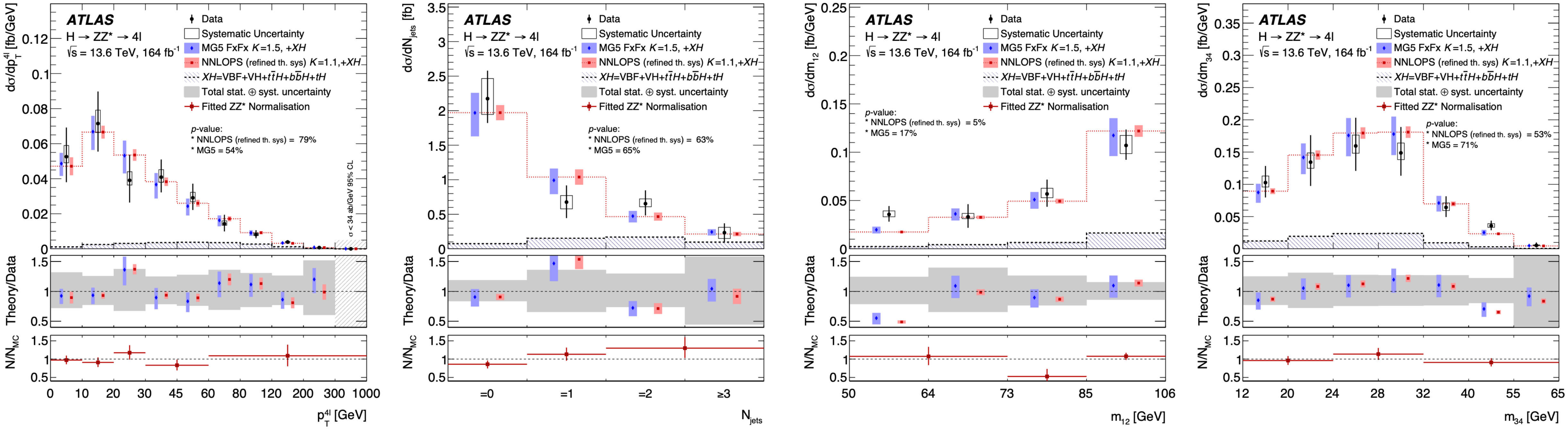

Differential Cross-Section Results

- Differential fiducial cross-section measurements for $p_T^{4\ell}$, N_{jets}, m_{12}, m_{34}, $\boldsymbol{y_{4\ell}}$**,** $\boldsymbol{\Delta\phi_{\text{jj}}}$**,** $\boldsymbol{\phi}$**, and 2D** $\boldsymbol{p_T^{4\ell}}$ **vs** $\boldsymbol{m_{34}}$
- **Good agreement with predicted XS observed across all bins**
  - MG5 and NNLO predictions normalised to the YR4 N3LO cross-section for ggF

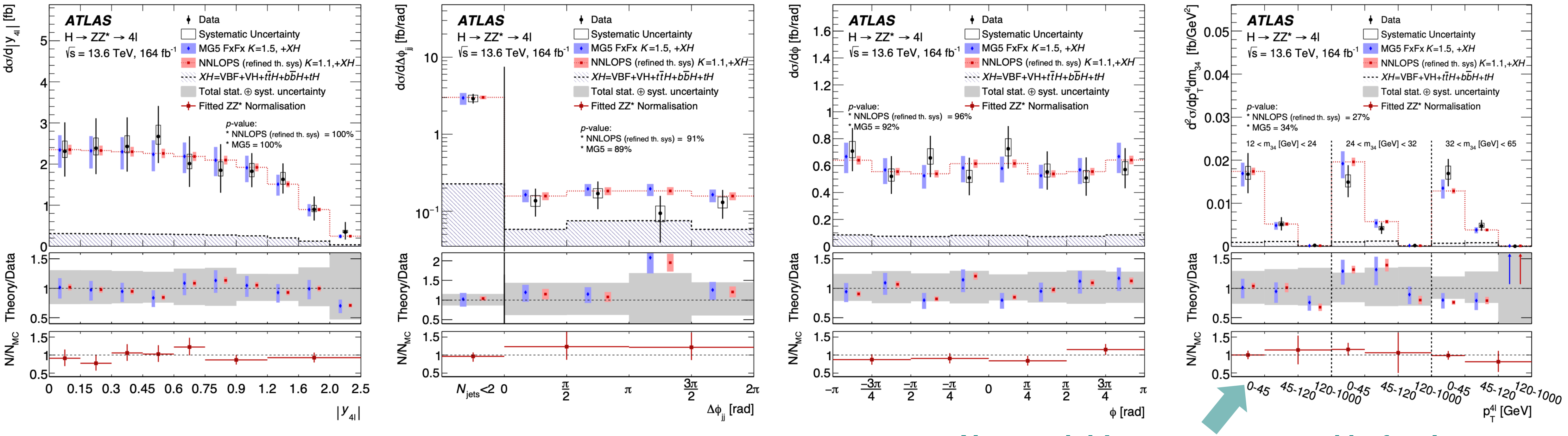

New variable never measured before!

Correlation matrices

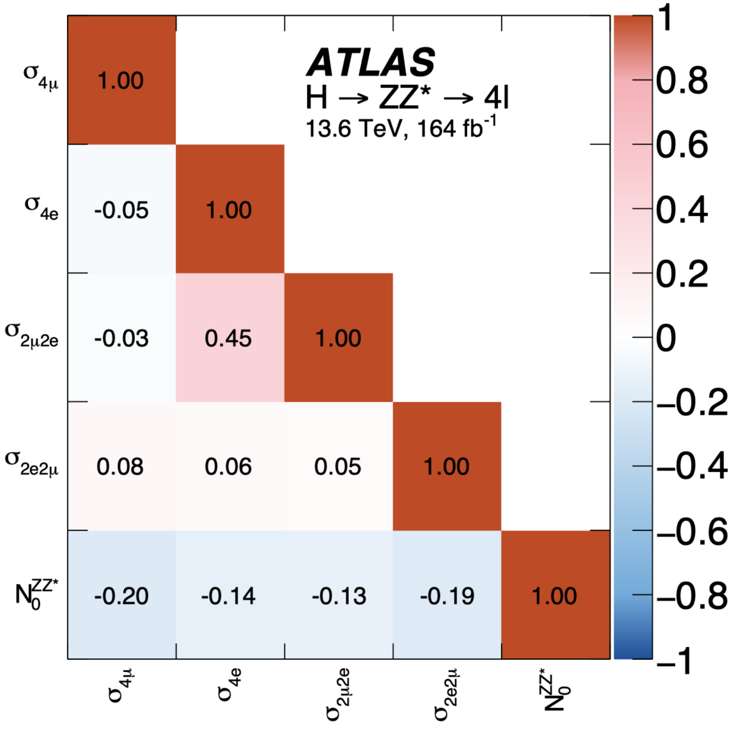

Per channel fit

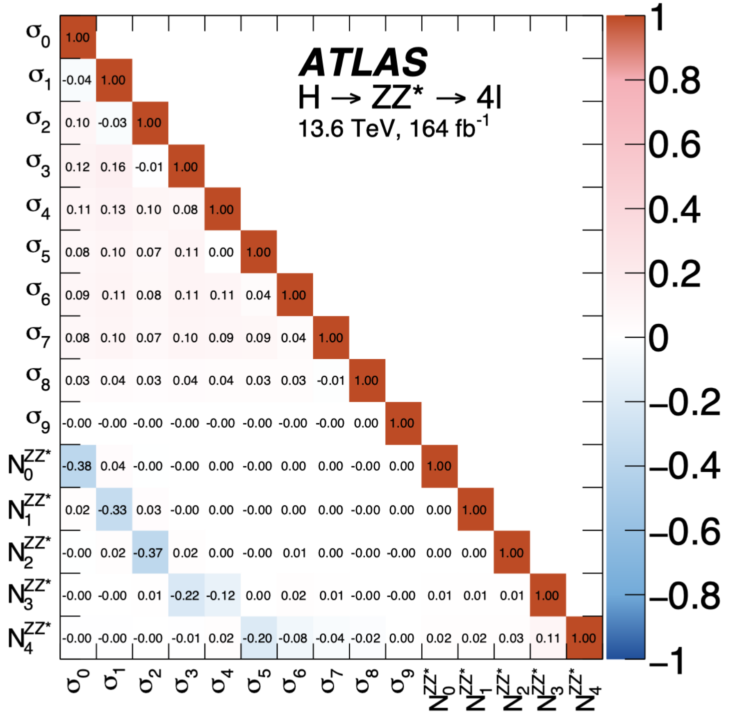

$p_T^{4\ell}$

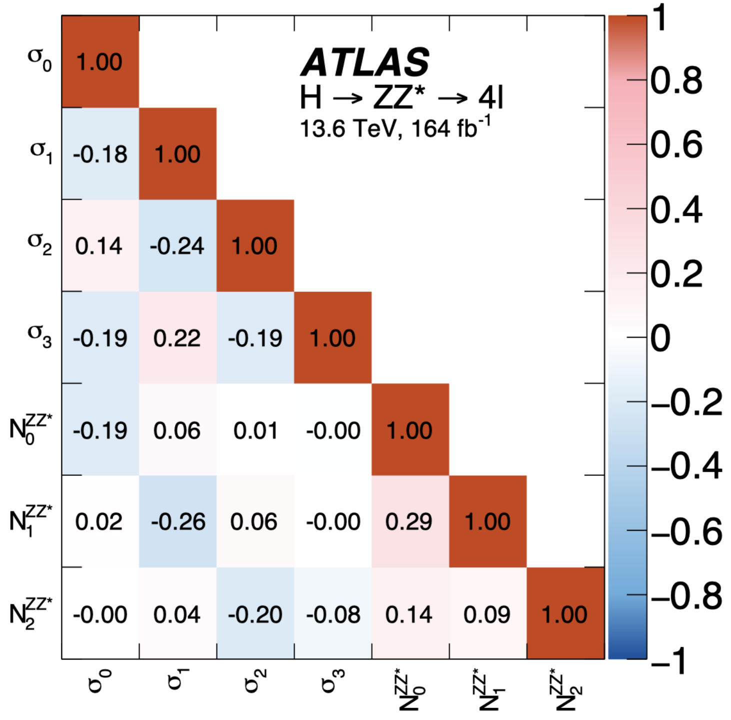

$N_{\rm jets}$

Correlation matrices

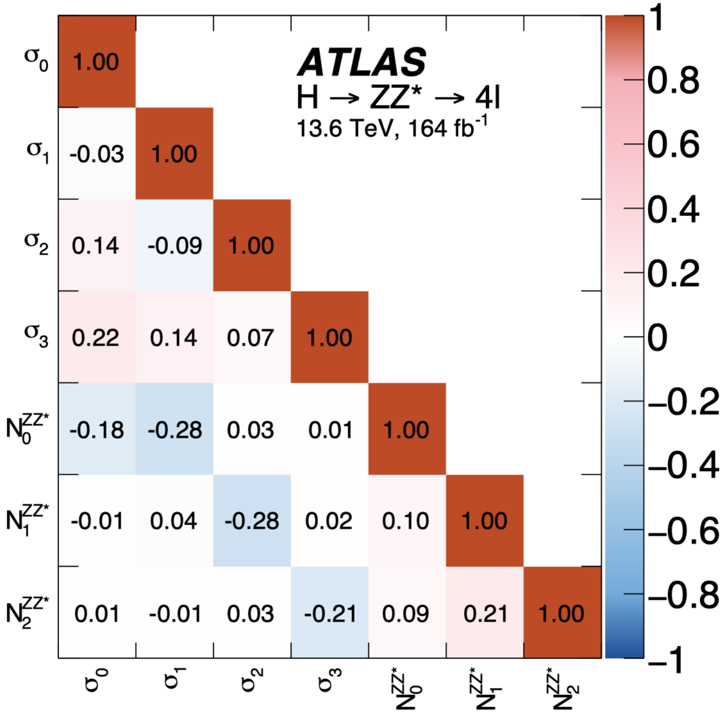

m_{12}

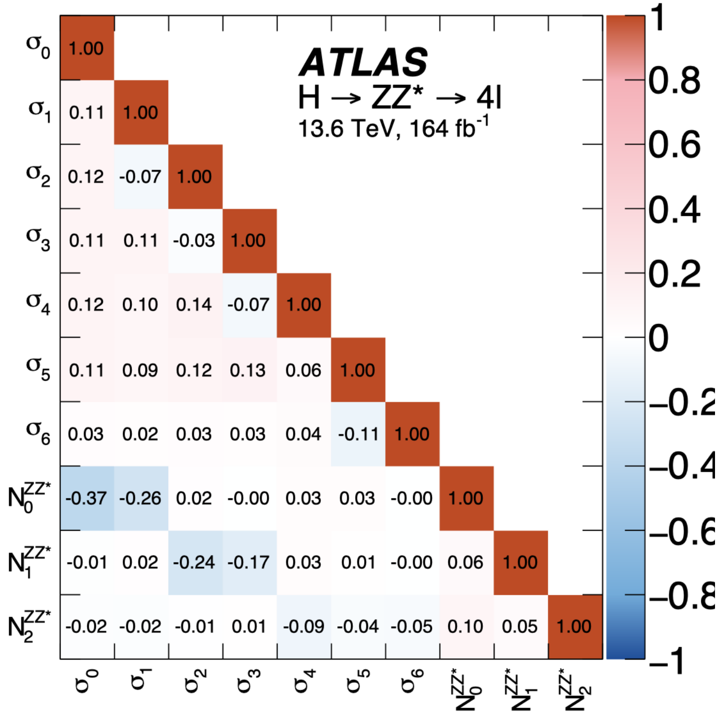

m_{34}

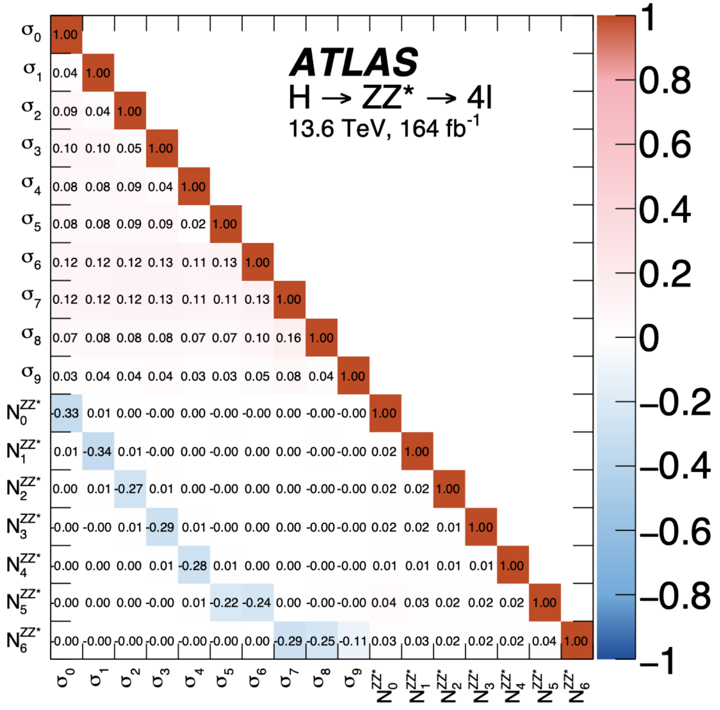

$y_{4\ell}$

Correlation matrices

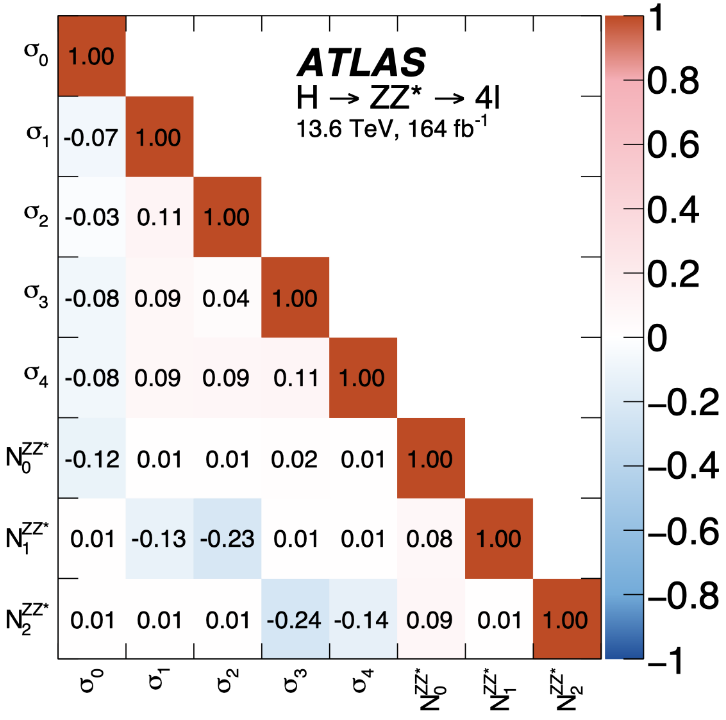

$\Delta\phi_{jj}$

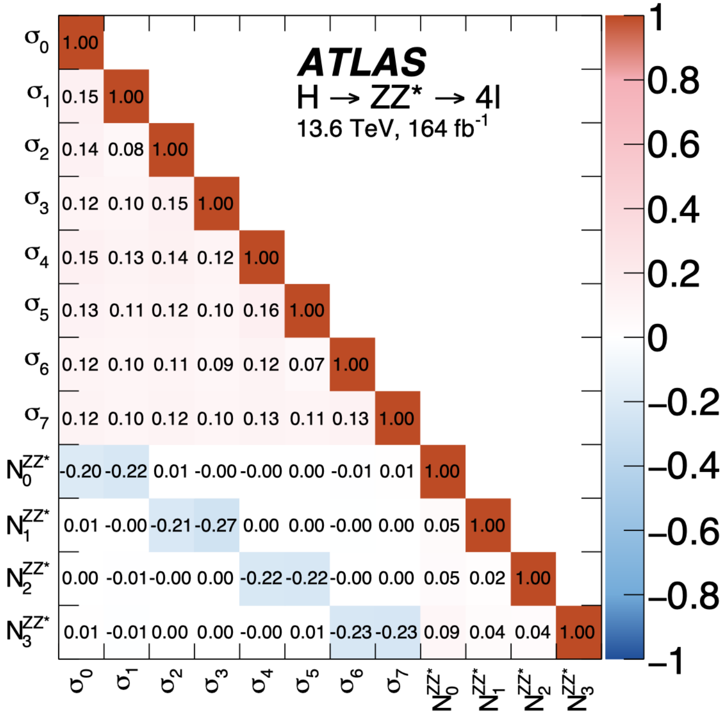

ϕ

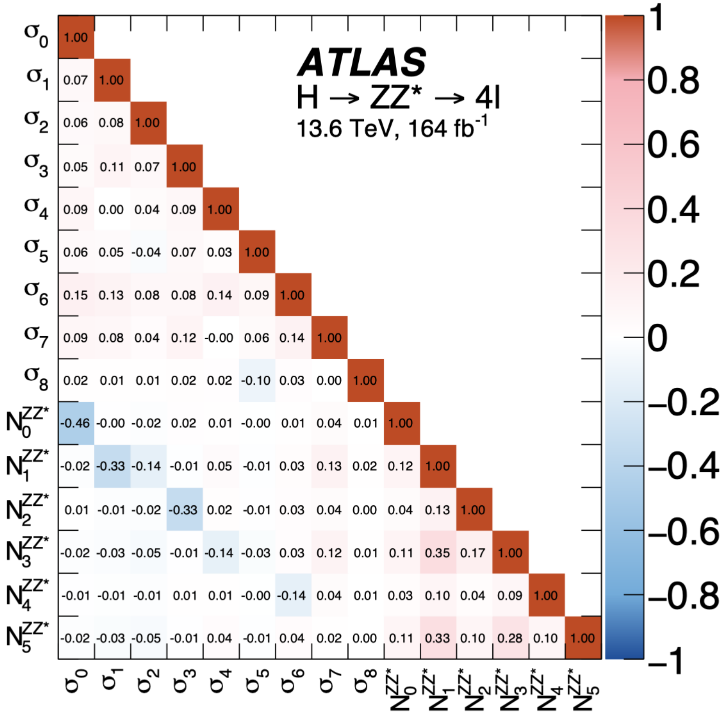

$p_T^{4\ell}$ vs m_{34}

SMEFT Interpretation – More details

Approach

- Generate EFT samples for different Wilson Coefficients (WCs) values
- Apply fiducial cuts to obtain fiducial differential distributions in each simulated scenario
- Extract differential EFT parametrisation in fiducial phase space and reparametrise SM workspace with SMEFT
- Perform likelihood scans across differential bins to set limits on WC values.

  → **Linear** vs **linear+quadratic** fits probe the robustness of SMEFT limits

  CP-even scans performed using m_{34}, ϕ, and 2D $p_T^{4\ell} m_{34}$
  CP-odd scans performed using ϕ and $\Delta\phi_{jj}$

$$\mathcal{L}_{\rm EFT} = \mathcal{L}_{\rm SM} + \sum_i \frac{C_i^{(d)}}{\Lambda^{(d-4)}} O_i^{(d)} \quad \text{for } d > 4$$

Operator	Structure	Coeff.
O_{HW}	$HH^\dagger W^l_{\mu\nu} W^{\mu\nu l}$	c_{HW}
O_{HB}	$HH^\dagger B_{\mu\nu} B^{\mu\nu}$	c_{HB}
O_{HWB}	$HH^\dagger \tau^l W^l_{\mu\nu} B^{\mu\nu}$	c_{HWB}
$O_{H\tilde{W}}$	$HH^\dagger \tilde{W}^l_{\mu\nu} W^{\mu\nu l}$	$c_{H\tilde{W}}$
$O_{H\tilde{B}}$	$HH^\dagger \tilde{B}_{\mu\nu} B^{\mu\nu}$	$c_{H\tilde{B}}$
$O_{H\tilde{W}B}$	$HH^\dagger \tau^l \tilde{W}^l_{\mu\nu} B^{\mu\nu}$	$c_{H\tilde{W}B}$

More technically

Wilson coefficients (Warsaw basis) constrained by comparing the unfolded signal cross-section in each bin of the chosen distribution to the SMEFT expectation

- Expected cross-section and acceptance parametrised using a matrix-element-based procedure:
  - for a bin j of a given observable, the expected cross-section is written as

$$\sigma^{\rm SMEFT}_{pp\to H\to 4\ell,j}(c_i) = \sigma^{\rm SM}_{pp\to H\to 4\ell,j}\cdot \sum_p \left(1+\sum_i \alpha_i^{(p,j)} c_i + \sum_{i,k\ge i}\beta_{ik}^{(p,j)} c_i c_k\right)\cdot \frac{\left(1+\sum_i \alpha_i^{(\Gamma_{4\ell},j)} c_i+\sum_{i,k\ge i}\beta_{ik}^{(\Gamma_{4\ell},j)} c_i c_k\right)}{\left(1+\sum_i \alpha_i^{(\Gamma_{tot},j)} c_i+\sum_{i,k\ge i}\beta_{ik}^{(\Gamma_{tot},j)} c_i c_k\right)}$$

Higgs boson production processes

obtained from matrix elements computed using dedicated simulated samples

Helicity suppression

If SM amplitude has a different helicity configuration that SMEFT amplitude, the integrated/inclusive contribution SM-SMEFT interference will be (approximately) zero

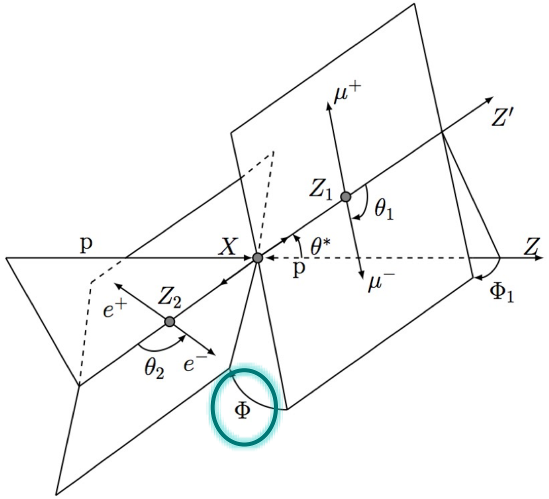

- ϕ is sensitive to the helicity structure of the Zs → can project out the interference pattern, even if it integrates to zero in helicity-inclusive observables
  - SMEFT simulation shows sign-changing modulations in ϕ very similar to the ones described for the SM processes
    - Phys. Rev. D 95 (2017)
    - Phys.Lett.B **776** (2018) 473
  - Other observables had suppressed SM-SMEFT interference contribution and were always quadratic dominated!
  - Same idea as CP interpretations. Look at CP odd observables to see the asymmetric effects that integrate to 0

- Gained sensitivity and more robust SMEFT interpretations
- We are pretty confident that helicity suppression is the underlying effect but would be nice to formalize the calculation as was done for the SM final states

SMEFT Interpretation – 1D Limits, CP-odd

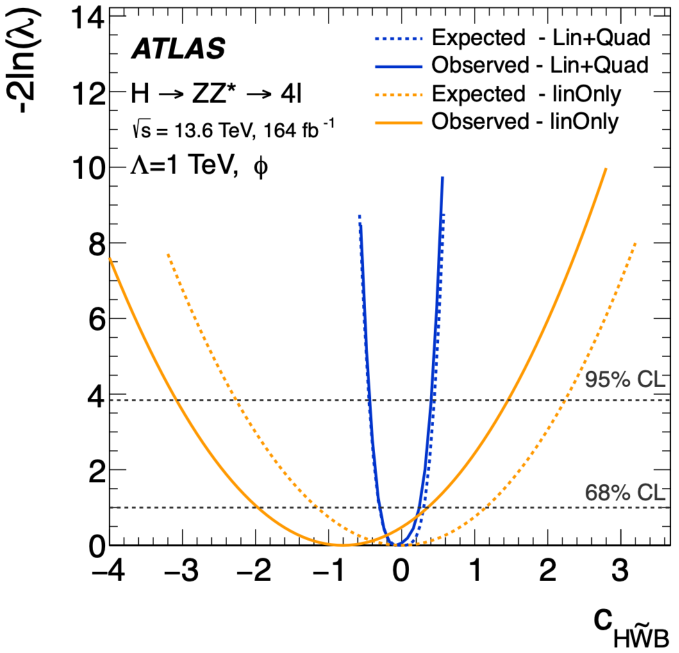

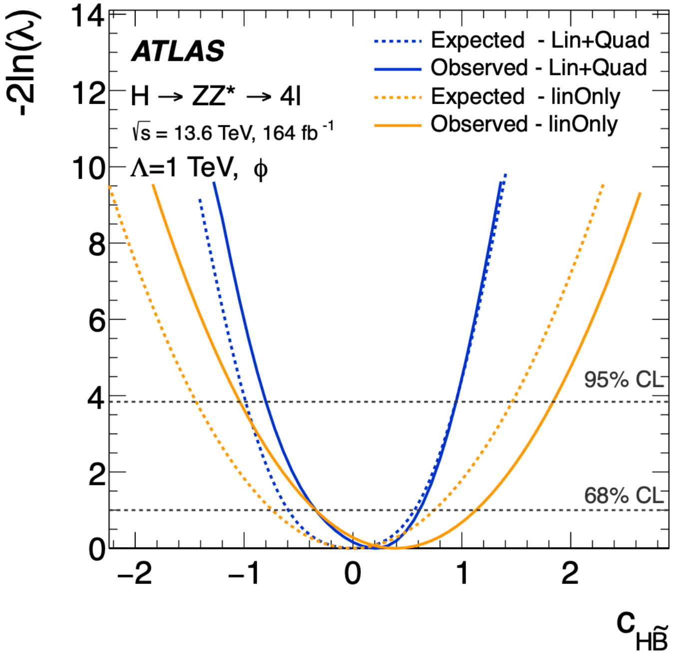

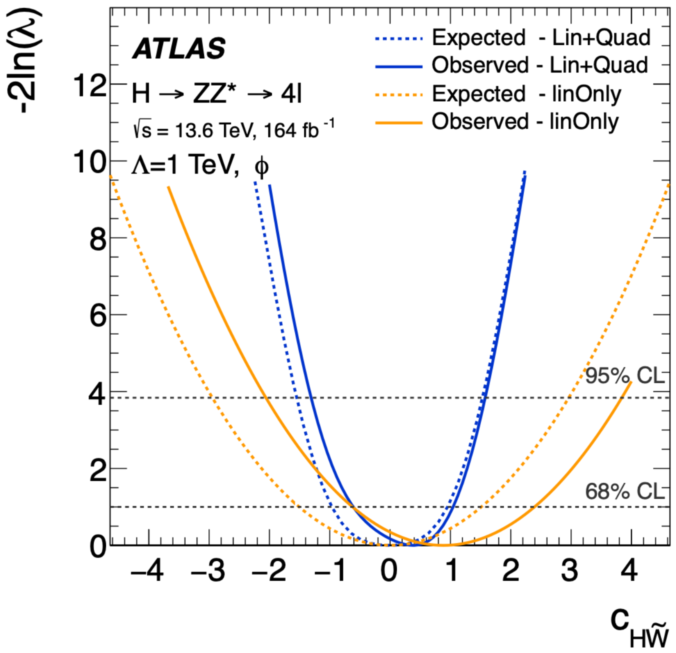

	Observable	Expected 95% CL [TeV^{-2}]		Observed 95% CL [TeV^{-2}]		Best fit [TeV^{-2}]	
		Linear	Linear + Quadratic	Linear	Linear + Quadratic	Linear	Linear + Quadratic
$c_{H\tilde{W}}$	Φ	$[-3.0, 3.0]$	$[-1.6, 1.6]$	$[-2.1, 3.9]$	$[-1.3, 1.6]$	0.88	0.38
	$\Delta\phi_{jj}$	–	$[-9.3, 9.4]$	–	$[-4.5, 5.4]$	-	0.23
$c_{H\tilde{B}}$	Φ	$[-1.5, 1.5]$	$[-1.0, 0.96]$	$[-1.1, 1.9]$	$[-0.80, 0.96]$	0.39	0.20
	$\Delta\phi_{jj}$	–	$[-1.5, 1.5]$	–	$[-0.92, 0.93]$	–	0.0023
$c_{H\tilde{W}B}$	Φ	$[-2.3, 2.3]$	$[-0.45, 0.45]$	$[-3.1, 1.5]$	$[-0.44, 0.41]$	-0.80	-0.089
	$\Delta\phi_{jj}$	–	$[-2.9, 2.9]$	–	$[-1.7, 1.7]$	–	-0.0066

SMEFT Interpretation – 1D Limits, CP-even

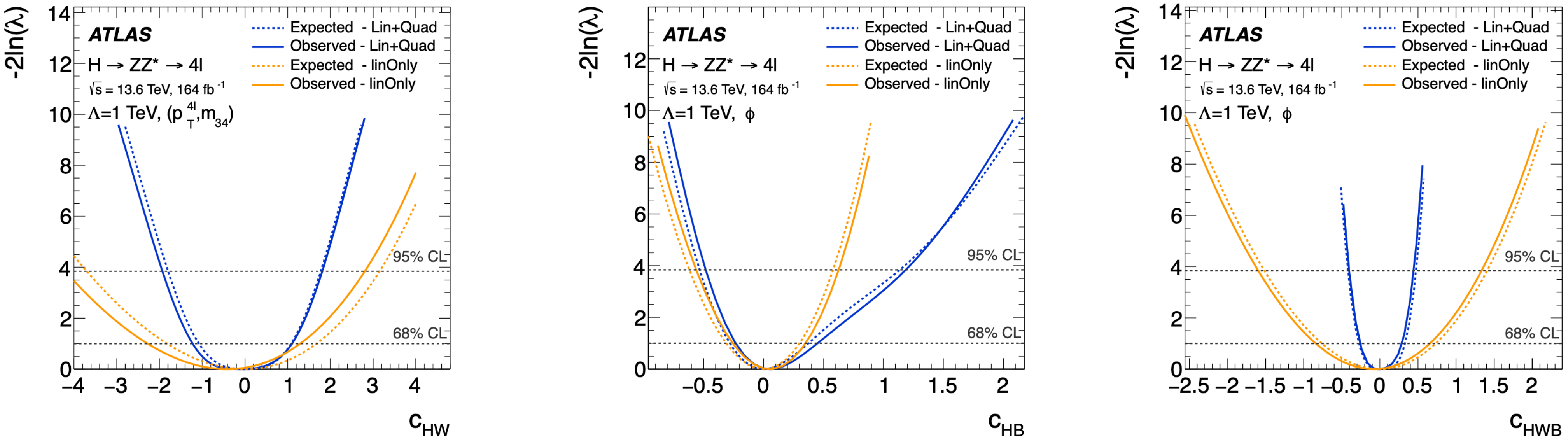

- Expected 95% CL reductions: c_{HW}: factor ~2, c_{HWB} : factor ~3.2
- Similar for CP-odd
- **c_{HB} is different:**
  - Limits similar in both treatments (interference-dominated)
  - Quadratic term slightly weakens sensitivity (~30%)

	Expected 95% CL [TeV^{-2}]		Observed 95% CL [TeV^{-2}]		Best fit [TeV^{-2}]	
	Linear	Linear + Quadratic	Linear	Linear + Quadratic	Linear	Linear + Quadratic
c_{HW}	[−3.8, 3.2]	[−1.8, 1.8]	[−4.3, 2.9]	[−2.0, 1.8]	-0.40	-0.08
c_{HB}	[−0.63, 0.59]	[−0.54, 1.2]	[−0.58, 0.64]	[−0.49, 1.25]	0.05	0.05
c_{HWB}	[−1.5, 1.4]	[−0.42, 0.48]	[−1.6, 1.3]	[−0.40, 0.45]	-0.08	-0.02
$c_{H\tilde{W}}$	[−3.0, 3.0]	[−1.6, 1.6]	[−2.1, 3.9]	[−1.3, 1.6]	0.88	0.38
$c_{H\tilde{B}}$	[−1.5, 1.5]	[−1.0, 0.96]	[−1.1, 1.6]	[−0.80, 0.96]	0.39	0.20
$c_{H\tilde{W}B}$	[−2.3, 2.3]	[−0.45, 0.45]	[−3.1, 1.5]	[−0.44, 0.41]	-0.80	-0.09

SMEFT Interpretation – 2D Limits

Two-dimensional likelihood scans are performed **to explore correlations** (third WC set to zero)

CP-even

CP-odd

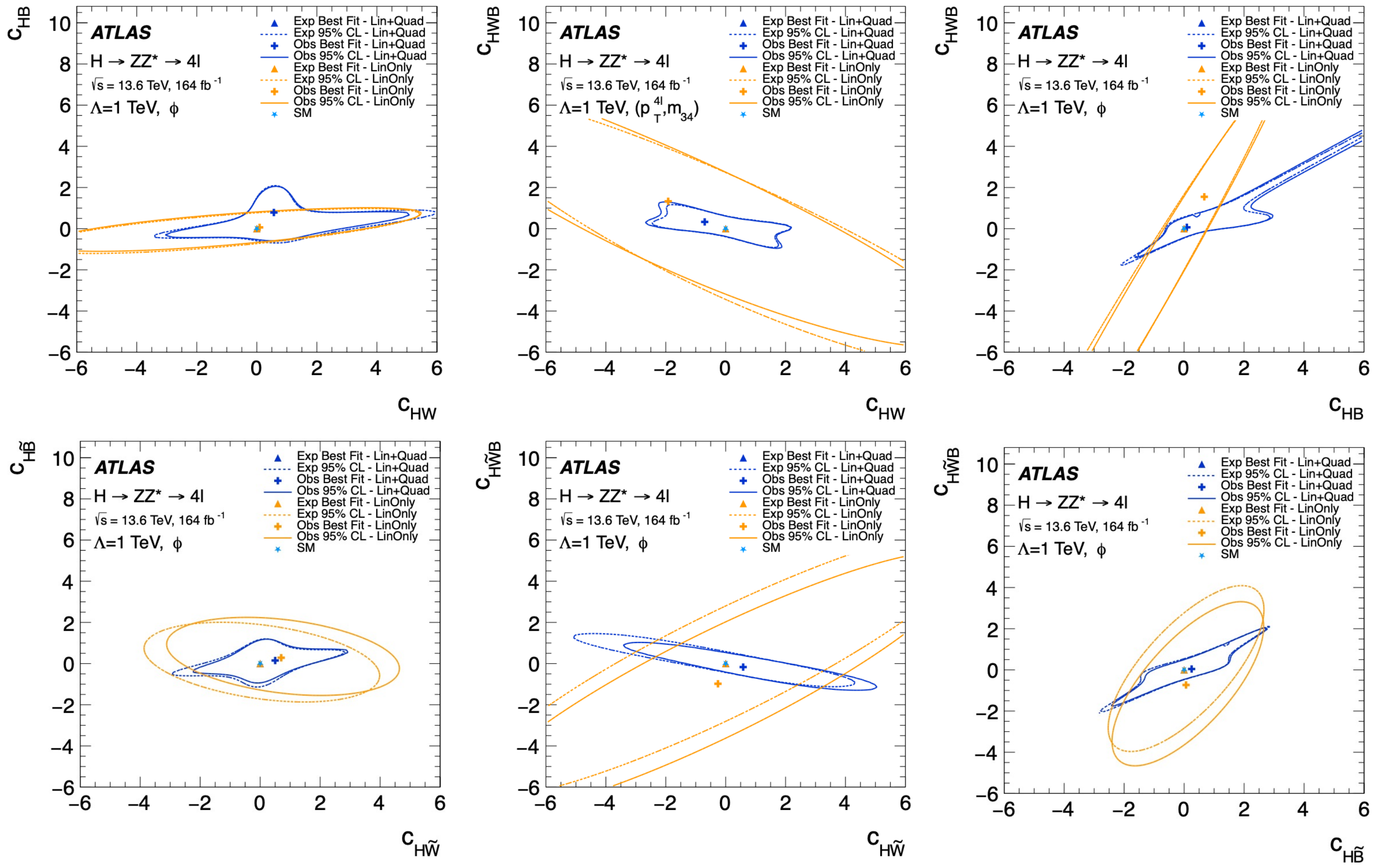

- **Linear-only** contours often show strong correlations with **flat directions (no 95%CL)**
- Including **quadratic** breaks flat directions (most of the sensitivity is from BSM-squared)